Supporting Information

Vighi et al. 10.1073/pnas.1718792115

SI Materials and Methods

General Experimental Methods for the Synthesis of cGMP Analogs. All applied solvents and reagents were available from commercial suppliers. Solvents used were specified as analytical or HPLC grade. DMSO was stored over activated molecular sieves for at least 2 wk before use. Chromatographic operations were performed at ambient temperature. Both reaction progress and purity of isolated products were determined by reversed-phase HPLC (RP-18, ODS-A-YMC, 120-S-11, 250 × 4 mm, 1.5 mL/min), wherein UV detection was performed either at 263 nm, an intermediate wavelength suitable to detect most cGMP products and impurities, or at the λ_{max} (wavelength at which absorbance is highest) of the given starting material or product. Syntheses were typically performed in a 20- to 200-μmol scale in 2-mL polypropylene reaction vials with screw cap [reactions requiring inert gas atmosphere and/or degassing were performed in round-bottom flasks (typically 10 or 25 mL)]. Dissolution of poorly soluble reactants was achieved through sonification or heating (70 °C) before addition of reagents. In case dissolution was not elicited by these techniques, which mainly applied to some cGMP analogs carrying a PET moiety, the suspension was used. Purification of products was accomplished by preparative reversed-phase HPLC (RP-18, ODS-A-YMC, 12 nm-S-10, 250 × 16 mm, UV 254 or 280 nm). The eluent composition is described in the synthetic examples and, unless stated otherwise, can be used for analytical purposes as well. Desalting of products was accomplished by repeatedly freeze drying or by preparative reversed-phase HPLC (RP-18, ODS-A-YMC, 12 nm-S-10, 250 × 16 mm, UV 254 or 280 nm) according to standard procedures for nucleotides. Solutions were frozen at −70 °C for 15 min before evaporation, in case a SpeedVac concentrator was used to remove the solvent. Products were either isolated as sodium or triethylammonium salt, depending on the applied buffer. Yields refer to the fraction of isolated product featuring the reported purity. They were calculated from UV absorbance at the λ_{max}, measured on a JASCO V-650 spectrophotometer (JASCO Germany GmbH) according to Lambert–Beer's law. Extinction coefficients were estimated from published values of structurally related compounds. Mass spectra were obtained with an Esquire LC 6000 spectrometer (Bruker Daltronics) in the electrospray ionization mass spectrometry (ESI-MS) mode with 50% water/50% methanol as matrix. CN01–CN04 and R_P-8-Br-cGMPS were prepared according to methods previously described (1). For CN03 PKG binding data see ref. 2. For a listing of analog codes, acronyms, and nomenclature used, refer to Table S1.

Preparation of 8-Thio-Substituted Guanosine-3′,5′-Cyclic Monophosphorothioate Analogs.

General procedure A. The corresponding thiol reactant (8 eq) and NaOH (2 M, 4 eq) were added successively to a solution of the corresponding 8-Br-substituted equatorially modified R_P-cGMPS analog (sodium salt, 65 mM, 1 eq) in H_2O:isopropanol (1:1, vol/vol). The reaction mixture was heated to 90 °C and stirred until the bromide starting material was completely consumed or no further reaction progress was observed. The solution was then allowed to reach room temperature and neutralized with HCl (1 M) and the solvent was removed through high-vacuum evaporation with a SpeedVac concentrator. The residue was dissolved in water (1 mL) and washed with tert-butyl methyl ether (3×). In case the residue was not water-soluble, the obtained suspension was washed with tert-butyl methyl ether and (if necessary) diluted with methanol to dissolve remaining precipitate. The aqueous phase was evaporated under reduced pressure using a rotary evaporator, the residue redissolved in water, subjected to preparative reversed-phase HPLC, and desalted, giving the 8-thio-substituted R_P-cGMPS analog.

General procedure B. The thiol(ate) reactant (4.5 eq) was added to a solution of the corresponding 8-Br-substituted R_P-cGMPS analog (sodium salt, 65 mM, 1 eq) in H_2O:isopropanol (1:1, vol/vol). The reaction mixture was stirred at room temperature until the bromide starting material was completely consumed or no further reaction progress was observed. The solution was then adjusted to pH 6 with NaOH (10%) and the solvent was removed through high-vacuum evaporation with a SpeedVac concentrator. The residue was dissolved in water (1 mL) and washed with CH_2Cl_2 (3×). The aqueous phase was evaporated under reduced pressure using a rotary evaporator, the residue redissolved in water, subjected to preparative reversed-phase HPLC, and desalted, giving the 8-thio-substituted R_P-cGMPS analog.

General procedure C. NaOH (2 M, 16 eq) and the corresponding thiol reactant (8 eq) were added successively to a solution of the 8-Br-substituted cGMP analog (sodium salt, 200 mM, 1 eq) in borate buffer (100 mM, pH 12). The reaction mixture was heated to 90 °C and stirred until the bromide starting material was completely consumed or no further reaction progress was observed. The solution was then allowed to reach room temperature and neutralized with HCl (1 M). The solvent was removed under reduced pressure using a rotary evaporator. The residue was dissolved in water (1 mL), subjected to preparative reversed-phase HPLC, and desalted.

Preparation of 1, N^2-Functionalized Guanosine-3′,5′-Cyclic Monophosphorothioate Analogs (General Procedure D). The 1, 8-diazabicyclo[5.4.0]undec-7-ene (7 eq) and the corresponding 2-bromo-aceto-reactant (3.5 eq) were added successively to a solution of the corresponding R_P-cGMPS analog (50 mM, 1 eq) in DMSO. The reaction mixture was stirred under exclusion of light until the R_P-cGMPS analog starting material was completely consumed or no further reaction progress was observed. The solvent was removed through high-vacuum evaporation with a SpeedVac concentrator. The residue was dissolved in methanol (0.5 mL) and the pH adjusted to 6–7 with HCl (1 M). In case a precipitate was formed thereby, methanol was added to redissolve it. Otherwise, water was slowly added until all components just remained soluble (maximum H_2O:methanol = 5:1). The solution was subjected to preparative reversed-phase HPLC and desalted, giving the 1, N^2-etheno-functionalized R_P-cGMPS analog.

Formation of Amide Bonds with Guanosine-3′,5′-Cyclic Monophosphorothioate Analogs (General Procedure E). N, N-diisopropylethylamine (2.2 eq) and benzotriazole-1-yl-oxytripyrrolidinophosphonium hexafluorophosphate (1.1 eq) were added successively to a solution of the corresponding carboxylic acid-substituted R_P-cGMPS analog (100 mM in DMSO, 1 eq) and the bis-amino spacer (0.5 eq). The reaction mixture was stirred until the starting material was completely consumed or no further reaction progress was observed (usually <10 min). Water (100 μL) was added, stirring was continued for 10 min, and the solvent was removed through high-vacuum evaporation with a SpeedVac concentrator. The residue was dissolved in water (1 mL), if necessary the pH was adjusted to 6 with NaOH (2 M) or HCl (1 M), and the solution was washed with ethyl acetate (5×). The aqueous phase was evaporated under reduced pressure using a rotary evaporator, redissolved in water, subjected to preparative reversed-phase HPLC, and desalted, giving the coupled R_P-cGMPS analog.

CN05: 8-(4-hydroxyphenylthio)-β-phenyl-1,N^2-ethenoguanosine-3′,5′-cyclic monophosphorothioate, R_P-isomer (R_P-8-pHPT-PET-cGMPS). Using general procedure A, R_P-8-Br-PET-cGMPS was reacted with 4-mercaptophenol (6 eq) in the presence of NaOH (2 M, 2.5 eq) to give the title compound.

Yield (purity): 54% (>99%).

HPLC: 26% acetonitrile, 10 mM NaH_2PO_4 buffer, pH 6.8; for preparative HPLC polar by-products are first separated using 22% acetonitrile, 10 mM NaH_2PO_4 buffer, pH 6.8, before switching to the described eluent.

UV visible (UV-VIS): λmax = 274 nm (pH 7), ε = 40,000 (estimated).

ESI-MS (+): *m/z* calculated for $C_{24}H_{21}N_5O_7PS_2$ ($[M + H]^+$): 586.06, found: 586.

ESI-MS (−): *m/z* calculated for $C_{24}H_{19}N_5O_7PS_2$ ($[M - H]^-$): 584.05, found: 584.

CN06: 8-(4-isopropylphenylthio)-β-phenyl-1,N^2-ethenoguanosine-3′,5′-cyclic monophosphorothioate, R_P-isomer (R_P-8-pIPrPT-PET-cGMPS). Using general procedure A (with modifications as indicated), R_P-8-Br-PET-cGMPS was reacted with 4-isopropylthiophenol (4 eq) in the presence of NaOH (2 M, 1 eq) and N, N-diisopropylethylamine (2 eq) in H_2O:methanol (1:3) at 60 °C to give the title compound.

Yield (purity): 32% (>99%).

HPLC: 35% acetonitrile, 50 mM NaH_2PO_4 buffer, pH 7.

UV-VIS: λmax = 274 nm (pH 7), ε = 40,000 (estimated).

ESI-MS (+): *m/z* calculated for $C_{27}H_{27}N_5O_6PS_2$ ($[M + H]^+$): 612.11, found: 612.

ESI-MS (−): *m/z* calculated for $C_{27}H_{25}N_5O_6PS_2$ ($[M - H]^-$): 610.10, found: 610.

CN07: 8-bromo-(3-thiophen-yl-1,N^2-etheno)guanosine-3′,5′-cyclic monophosphorothioate, R_P-isomer [R_P-8-Br-(3-Tp)ET-cGMPS]. Using general procedure D, R_P-8-Br-cGMPS was reacted with 3-(bromoacetyl)-thiophene to give the title compound.

Yield (purity): 61% (>99%).

HPLC: 24% acetonitrile, 50 mM NaH_2PO_4 buffer, pH 6.8.

UV-VIS: λmax = 261 nm (pH 7), ε = 40,000 (estimated).

ESI-MS (+): *m/z* calculated for $C_{16}H_{14}BrN_5O_6PS_2$ ($[M + H]^+$): 545.93, found: 546.

ESI-MS (−): *m/z* calculated for $C_{16}H_{12}BrN_5O_6PS_2$ ($[M - H]^-$): 543.92, found: 544.

CN08: 8-(2-aminophenylthio)guanosine-3′,5′-cyclic monophosphorothioate, R_P-isomer (R_P-8-oAPT-cGMPS). Using general procedure B, R_P-8-Br-cGMPS was reacted with 2-aminothiophenol to give the title compound.

Yield (purity): 47% (>99%).

HPLC: 40% methanol, 20 mM triethylammonium formate buffer, pH 6.8.

UV-VIS: λmax = 278 nm (pH 7), ε = 18,000 (estimated).

ESI-MS (+): *m/z* calculated for $C_{16}H_{18}N_6O_6PS_2$ ($[M + H]^+$): 485.05, found: 485.

ESI-MS (−): *m/z* calculated for $C_{16}H_{16}N_6O_6PS_2$ ($[M - H]^-$): 483.03, found: 483.

Precursor for synthesis of CN09: 8-carboxymethylthioguanosine-3′,5′-cyclic monophosphorothioate, R_P-isomer (R_P-8-CMT-cGMPS). Using general procedure C, R_P-8-Br-cGMPS was reacted with mercaptoacetic acid to give the title compound (Fig. S5).

Yield (purity): 74% (>99%).

HPLC: 4% acetonitrile, 30 mM NaH_2PO_4 buffer, pH 6.8.

UV-VIS: λmax = 275 nm (pH 7), ε = 13,700 (estimated).

ESI-MS (+): *m/z* calculated for $C_{12}H_{16}N_5O_8PS_2$ ($[M + H]^+$): 453.02, found: 453.

ESI-MS (−): *m/z* calculated for $C_{12}H_{14}N_5O_8PS_2$ ($[M - H]^-$): 451.00, found: 451.

CN09: guanosine-3′,5′-cyclic monophosphorothioate[R_P]-[8- thiomethylamido-(octaethoxy)-ethylamidomethylthio-8]-guanosine-3′,5′-cyclic monophosphorothioate[R_P] [R_P-cGMPS-8-TMAmd-(EO)$_8$-EAmdMT-8- R_P-cGMPS]. Using general procedure E, the precursor compound R_P-8-CMT-cGMPS was reacted with NH_2-PEG_8-$CH_2CH_2NH_2$ to give the title compound.

Yield (purity): 26% (>99%).

HPLC: 14% acetonitrile, 50 mM NaH_2PO_4 buffer, pH 6.8.

UV-VIS: λmax = 275 nm (pH 7), ε = 24,660 (estimated).

ESI-MS (+): *m/z* calculated for $C_{42}H_{65}N_{12}O_{22}P_2S_4$ ($[M + H]^+$): 1,279.27, found: 1,279.

ESI-MS (−): *m/z* calculated for $C_{42}H_{63}N_{12}O_{22}P_2S_4$ ($[M - H]^-$): 1,277.25, found: 1,277.

Precursor for synthesis of CN10: 8-carboxymethylthio-β-phenyl-1,N^2-ethenoguanosine-3′,5′-cyclic monophosphorothioate, R_P-isomer (R_P-8-CMT-PET-cGMPS). Using general procedure C, R_P-8-Br-PET-cGMPS was reacted with mercaptoacetic acid to give the title compound (Fig. S6).

Yield (purity): 75% (>99%).

HPLC: 17% acetonitrile, 30 mM NaH_2PO_4 buffer, pH 6.8; for preparative HPLC polar by-products are first separated using 10% acetonitrile, 30 mM NaH_2PO_4 buffer, pH 6.8, before switching to the described eluent.

UV-VIS: λmax = 273 nm (pH 7), ε = 40,000 (estimated).

ESI-MS (+): *m/z* calculated for $C_{20}H_{19}N_5O_8PS_2$ ($[M + H]^+$): 552.04, found: 552.

ESI-MS (−): *m/z* calculated for $C_{20}H_{17}N_5O_8PS_2$ ($[M - H]^-$): 550.03, found: 550.

CN10: β-phenyl-1,N^2-ethenoguanosine-3′,5′-cyclic monophosphorothioate[R_P]-[8- thiomethylamido-(octaethoxy)-ethylamidomethylthio-8]-β-phenyl-1,N^2-ethenoguanosine-3′,5′-cyclic monophosphorothioate[R_P] [PET-R_P-cGMPS-8-TMAmd-(EO)$_8$-EAmdMT-8-R_P-cGMPS-PET]. Using general procedure E, the precursor compound R_P-8-CMT-PET-cGMPS was reacted with NH_2-PEG_8-$CH_2CH_2NH_2$ to give the title compound.

Yield (purity): 57% (>99%).

HPLC: 25% acetonitrile, 80 mM NaH_2PO_4 buffer, pH 6.8.

UV-VIS: λmax = 272 nm (pH 7), ε = 72,000 (estimated).

ESI-MS (+): *m/z* calculated for $C_{58}H_{73}N_{12}O_{22}P_2S_4$ ($[M + H]^+$): 1,479.33, found: 1,479.

ESI-MS (−): *m/z* calculated for $C_{58}H_{71}N_{12}O_{22}P_2S_4$ ($[M - H]^-$): 1,477.32, found: 1,477.

Determination of Compound Lipophilicity. Although a generally accepted indicator for the expected capability of a given analog to pass through the cellular lipid bilayer by passive diffusion is the octanol/water partition coefficient log P, the determination of such data is rather difficult for polar structures such as cyclic nucleotides. Lipophilicity information is thus often only obtained by fragment analysis and corresponding calculations.

An established HPLC method, which is based on retention data on RP-18 reversed-phase silica (3) during gradient elution, was used for the determination of lipophilicity. Instead of log P the method yields the descriptor log k'_g, also ranking analytes according to their lipophilicity on a logarithmic scale. Since charged molecules, such as cyclic nucleotides, are only poorly retained on reversed phases, ion pair chromatography with the lipophilic triethylammonium cation was used.

Unmodified cGMP itself (log k'_g 0.77) is considered not to be membrane-permeant by passive diffusion, which means that only analogs with considerable hydrophobic modifications and substituents, respectively, which counteract against the negative charge at the phosphate moiety, can be used for extracellular application. A prior analysis of widely used cyclic nucleotide analogs in our laboratory has shown that noteworthy diffusion into cells takes place only for analogs having a log k'_g of at least 1.2, in line with previous data (4).

The corresponding data for 10 R_P-cGMPS analogs is shown in Table 1. For comparison and control, three established structures (compounds A, B, and C) were reanalyzed within this series. All monomeric analogs had log k'_g values > 1.2 (rL_{cGMP} > 2.7) and thus have sufficient lipophilicity to cross cellular membranes per se. Since the two cGMPS dimers (CN09 and CN10) carry two negative charges at physiological pH, the corresponding values are not directly comparable with log k'_g values obtained for the monomeric analogs with only a single negative charge.

Production of GSH-Conjugated Liposomes Encapsulating CN03. First, micelles were prepared by mixing (molar ratio 1:1.5) DSPE-PEG2000-maleimide [916 mg in 36.72 mL of deionized (DI) water; NOF America Corp.] with glutathione (144 mg in 4.42 mL of DI water; Sigma-Aldrich) at room temperature for 2 h. Next, micelles were added to Ca^{2+} acetate hydrate (4,094 mg in 57.36 mL of DI water; final concentration 200 mM) and kept at 60 °C for 30 min.

An amount of 2.808 mg of HSPC (hydrogenated soy phosphatidylcholine; final concentration 28 mM) and 912 mg of cholesterol (final concentration 18.6 mM) were dissolved in 30.96 mL ethanol in a serum bottle, mixed with the micelles while stirring, and incubated in a water bath for 30 min at 60 °C. Finally, the liposomes were extruded using 0.2/0.2 μm polycarbonate (PC) membrane (two times), 0.2/0.1 μm PC membrane (two times), and 0.1/0.1 μm PC membrane (two times) at 60 °C and stored at 4 °C. The size of liposomes was measured with 10 μL of the liposomal suspension diluted in 1 mL PBS by the dynamic light scattering method (Zetasizer Nano ZS). The average size of the liposome batches was between 100 and 120 nm, polydispersity index < 0.1. After size was measured the Ca^{2+} acetate liposomes were purified from nonencapsulated Ca^{2+} acetate hydrate using the TFF dialysis system (Millipore Cogent μScale and Millipore Pellicon cassette 50 cm^2). The liposomes were dialyzed against seven volumes of saline (0.9% NaCl). The batch was concentrated back to start volume 120 mL using dialysis with a TFF system and analyzed for lipid content and size.

LP-CN03 was generated by remote loading of the Ca^{2+} acetate GSH-PEG-liposomes with CN03 at a drug/phospholipid molar ratio 0.3. For this, 1 vol of CN03 dissolved in MilliQ (40 mg/mL) was mixed with 9 vol of liposomes (HSPC 20 mg/mL, both prewarmed at 60 °C) and incubated at 60 °C for 45 min. Subsequently, the batch was stored at 4 °C, purified, and analyzed. Purification was done by dialysis using a TFF system. The LP-CN03 liposomes were dialyzed against 10 vol of saline, concentrated to a CN03 concentration of 3 mg/mL, and sterile-filtered with a 0.2-μm filter (Corning sterile syringe filter) and stored at 4 °C. Encapsulated CN03 (i.e., LP-CN03) and other liposome constituents were analyzed by HPLC.

Animals. Animals for preparation of primary retinal cell cultures were kept at Centro Servizi Stabulario Interdipartimentale of the University of Modena and Reggio Emilia. The protocol was approved by the Ethical Committee of the University of Modena and Reggio Emilia (protocol no. 106 22/11/2012) and by the Italian Ministero della Salute (346/2015-PR). Animals for in vitro retinal explant studies were kept at the animal facilities of the Biomedical Centre, Lund University. Here, we used the C3H *rd1*/*rd1* (*rd1*), C3H *rd2*/*rd2* (*rd2* or *rds*), and C57Bl6J *rd10*/*rd10* (*rd10*) *Retinitis Pigmentosa* model mice and, when applicable, corresponding WT controls (Table S2). Animals were kept under standard white cyclic lighting, with ad libitum access to food and water, and were used irrespective of sex. All procedures were evaluated by the local animal care and ethics committees and performed in accordance with permits M172-12, M191-14, and M92-15. Efforts were made to keep the number of animals used and their suffering to a minimum.

Animals for in vivo studies were kept in the Tübingen Institute for Ophthalmic Research animal housing facility, under standard white cyclic lighting, had free access to food and water, and were used irrespective of sex unless stated otherwise. *rd1* and control C3H WT mice were used for initial in vivo testing. After successful testing in *rd1* animals, further in vivo cross-model validation was performed in *rd2* and *rd10* mice. Initial toxicity testing was done in C3H WT mice and CD WT rats. All in vivo procedures were performed in accordance with the local ethics committee at Tübingen University (§4 registrations from 29 to 04-10; 30-06-10; 11-03-11; animal permit AK5/12) and the Association for Research in Vision and Ophthalmology statement for the use of animals in ophthalmic and visual research.

Mice and rats dosed with LP-CN03 intraperitoneally, as well as their untreated controls, were routinely examined in vivo and postmortem. Treated animals in vivo showed no alterations in behavior (e.g., anxiety, apathy, or hunched, kyphotic posture), in the appearance of fur (e.g., hair loss or oily fur), or their skin (e.g., discolorations or hemorrhages). In vivo eye examinations found no abnormalities (e.g., lens opacity or cataract), while functional ERG testing revealed equal or better performance in LP-CN03–treated animals compared with untreated controls. Treated and untreated animals showed normal weight gains during their first two postnatal months (Fig. S3 *E* and *F*) and were generally undistinguishable from each other. Likewise, macroscopic postmortem examination of internal organs (heart, liver, lungs, kidney, and brain) revealed no abnormalities (organ size and form or coloration/perfusion) in LP-CN03–treated mice and rats.

Primary Photoreceptor-Like Cell Cultures: Preparation, Differentiation, and Treatments. Primary culture of photoreceptor-like retinal cells were derived from WT or *rd1* murine eyes as previously described (5, 6). About 20% of the primary cells can be differentiated into rod photoreceptors when exposed to 1% FBS and a subset of these express CNGC (7). Photoreceptor-like cells were differentiated from retinal neurospheres isolated from the ciliary epithelium of adult WT and *rd1* mice after treatment with 2 mg/mL dispase (20 min) followed by 1.33 mg/mL trypsin, 0.67 mg/mL hyaluronidase, and 0.13 mg/mL kynurenic acid (10 min) and cultured for a week in serum-free medium DMEM-F12 (Thermo Fisher Scientific) containing 20 ng/mL basic FGF, 2 μg/mL heparin, 0.6% glucose, and N2 hormone mix (Thermo Fisher Scientific). Retinal neurospheres were plated on glass slides coated with ECM (Sigma) and cultured in DMEM-F12 supplemented with 20 ng/mL FGF for 4 d. Cells were then allowed to differentiate in DMEM-F12 supplemented with 1% FBS. *rd1* differentiated photoreceptor-like cells activated a cell death program at the 11th day of differentiation (DIV11), as previously published (6). Cells were exposed to different doses of compounds at DIV10 (1 d before the peak of cell death) and, 18 h after treatment, cells were fixed with 4% paraformaldehyde (PFA) for 10 min at room temperature. Cell death was evaluated by staining for 2 min with 2 μM ethidium homodimer-1 (Life Technologies) and counterstaining

of nuclei with 0.1 μg/mL DAPI (Sigma). Slides were mounted with Mowiol 4-88 (Sigma) and analyzed at a Zeiss Axioskop 40 fluorescence microscope (Zeiss). Ethidium homodimer-1–positive, dying cells were counted on each slide and expressed as percentages of the total number of cells (DAPI-stained) per slide.

For Ca^{2+} ion measurements, Fluo-4 AM (Life Technologies) was loaded into either untreated or treated cells for 30 min at 37 °C in Ca^{2+}-free medium. Cells were fixed with 4% PFA for 10 min at room temperature and nuclei were stained with DAPI. Cells were analyzed with a Zeiss Axioskop 40 fluorescence microscope, as previously described (6). The fluorescence intensity of each cell was measured with ImageJ software in three slides from three biological replicates and the averaged intensities from at least 20 cells for each sample were plotted.

For calpain activity assays, differentiated cells grown on coverslips were incubated for 15 min in calpain reaction buffer (CRB: 25 mM Hepes-KOH, pH 7.2, 65 mM KCl, 2 mM $MgCl_2$, 1.5 mM $CaCl_2$, and 2 mM DTT) and then exposed for 1 h at 37 °C to the fluorescent calpain substrate CMAC, t-BOC-Leu-Met (A6520; Invitrogen) at a final concentration of 2 μM. Slides were washed twice for 10 min each in CRB, mounted with Mowiol 4-88, and analyzed at a Zeiss Axioskop 40 fluorescence microscope. The fluorescence intensity of each cell was measured with ImageJ software in three slides from three biological replicates and the averaged intensities from at least 20 cells from each sample were plotted.

For immunofluorescence, cells were fixed in 4% PFA. Cell death was detected by TdT-mediated dUTP terminal nick-end labeling kit (TUNEL, fluorescein; Roche) according to the producer's protocols. Primary antibodies were used as follows: anti-AIF (1:100; Sigma), anti-cGMP (1:250, from Jan de Vente and Harry Steinbusch, Maastricht University, Maastricht, The Netherlands), anti-Rho (1D4 1:1,000; Sigma), anti-Rho (R9153 1:250; Sigma), anti-PKG1α (1:100; Santa Cruz Biotechnologies), anti-PKG1β (1:100; Santa Cruz Biotechnologies), anti-PKG2 (1:100; Santa Cruz Biotechnologies), antiphosphorylated VASP-Ser239 (1:250; Nanotools, Antikörpertechnik), and antiphosphorylated VASP-Ser157 (1:250; Nanotools). Secondary antibodies were Alexa Fluor 568 or Oregon Green anti-goat, anti-mouse, anti-rabbit, and anti-sheep antibodies (Molecular Probes). Slides were mounted with Mowiol 4-88 (Sigma) and analyzed at a Zeiss Axioskop 40 fluorescence microscope. Nuclei were stained with 0.1 μg/mL DAPI (Sigma). The fluorescence intensity of each cell after staining with antiphosphorylated VASP-Ser239 and anti-cGMP antibodies was measured with ImageJ software in three slides from three biological replicates and the averaged intensities from at least 20 cells from each sample were plotted. The percentage of cells labeled with TUNEL and with nuclear translocated AIF was calculated in three slides from three biological replicates.

Organotypic Retinal Explant Cultures and Analysis of cGMP Analog Effects. Procedures were essentially as in Caffé et al. (8). In detail, P5 *rd1* animals were killed and the eyes rapidly enucleated in an aseptic environment. The entire eyes were incubated in R16 serum-free culture medium (07490743A; Invitrogen Life Technologies), with 0.12% proteinase K (193504; MP Biomedicals), at 37 °C for 15 min, to allow preparation of retinal cultures with retinal pigment epithelium (RPE) attached. The proteinase K was inactivated with 10% FCS (16000036; Gibco) in R16 medium, and thereafter the eyes were dissected aseptically in a Petri dish containing fresh R16 medium. A typical experiment had two rounds, with one round of experiments concerning three animals from the same litter, whose six eyes were put in the same vessel for the treatment above. The eyes were then randomly assigned to either no treatment (two) or treatment (four). The anterior segment, lens, vitreous, sclera, and choroids were carefully removed by fine scissors, and the retina was cut perpendicular to its edges, giving a cloverleaf-like shape. Subsequently, the retina was transferred to a Millicell culture dish filter insert (PIHA03050; Millipore AB) with the RPE layer facing the membrane. The insert was put into a six-well culture plate and incubated in R16 medium with supplements (9) at 37 °C. The full volume of nutrient medium, 1.5 mL per dish, was replaced with fresh medium every second day.

For the first 2 d the retina was cultured with R16 medium without treatment to allow it to adapt to culture conditions. cGMP analogs were dissolved in water, except for CN04–CN06, which were dissolved in DMSO at concentrations known not to affect retinal explant viability significantly (10). After 2 d (i.e., at P7), cultures were either exposed to different analogs or kept as untreated control (with addition of vehicle, if applicable). The cultures were stopped 4 d later [corresponding to P11, a time point when the *rd1* ONL has not shrunk in any appreciable way, permitting unbiased comparisons between treated and not treated explants (11)], by 2 h fixation in 4% PFA. This was followed by graded sucrose cryoprotection, embedding, and collecting of 12-μm-thick retinal cross-sections on a HM560 cryotome (Microm). This particular culturing paradigm is referred to as P5 + 2 + 4 d in vitro, DIV, thus ending up at P11. For the *rd2* model the corresponding scheme was P5 + 2 + 12 DIV, ending at P19, and for the *rd10* model we used either P7 + 2 + 8 DIV or P8 + 2 + 8 DIV, ending up as P17/P18, respectively. The outcomes of the two *rd10* schemes were indistinguishable by ANOVA and were hence used together. In the Fig. 4*F* legend the *rd10* data are referred to as P18 for convenience.

The various cGMP analogs were tested for their effect on photoreceptor cell death at a concentration of 50 μM (except CN05, tested at 10 μM), using TUNEL staining (based on In Situ Cell Death Detection Kit, 11684795910, red fluorescence; Sigma-Aldrich). DAPI (Vectashield Antifade Mounting Medium with DAPI; Vector Laboratories) was used as blue fluorescence nuclear counterstain. Three microscope slides were selected from three cutting levels (representing the central part of the explant plus positions ∼60 μm on each side of it), so as to avoid possible uneven distribution as well as cellular overlap in the staining. After the staining, each section of interest was photographed in both red and blue channel through the 20× objective of a Zeiss Axiophot fluorescence microscope (Zeiss), equipped with an Olympus DP70 digital camera (LRI Instruments). Each section gave rise to two photographs, one from one half of the section ("left") and one from the other half of the sections ("right"). The resulting images were then analyzed via the Fiji image analysis program (ref. 12; https://fiji.sc) by first determining the ONL. Red and blue channels were separated and after adjusting the threshold and minimum size of structures to be counted (via the "analyse particles" plug-in), the total number of TUNEL positive cells in the ONL was counted automatically and expressed as cells per 10,000 μm^2 ONL area.

In this way, each section gave rise to two values, left and right, which were averaged and taken as the entry for one particular section. This was repeated for each of the other two sections analyzed from each culture. The three separate section values were then averaged, to give one single value, which served as the final TUNEL-positive cells per 10,000 μm^2 (i.e., "TUNEL value") entry for a given explant. For each analog, an experiment typically consisted of six retinas from three animals, with four retinas randomly selected for treatment and two for no treatment. The whole experiment was then repeated to get observations from two independent litters, and to yield in total eight treated and four untreated explants, unless otherwise indicated.

For comparisons, the individual TUNEL value from each explant in the study of a certain analog was then recalculated to obtain so-called ratio values in the following way. First, the TUNEL values of the untreated explants were averaged. The TUNEL value from each treated explant was then compared with

this value and the ratio between them calculated. This produced a treated/untreated ratio that was either <1.0 if the treatment caused a reduction of the TUNEL value (i.e., cell death) or 1.0 or >1.0 if the treatment had no effect or increased the TUNEL value, respectively. The individual TUNEL values of the untreated explants in a given analog study were similarly compared with the average of the same, which allowed us to also depict the variation among the untreated specimens.

Ca^{2+} Imaging in Live Retinal Slice Preparations. For Ca^{2+} imaging experiments we used 3- to 8-wk-old HR2.1:TN-XL transgenic mice (13) that express the TN-XL Ca^{2+} biosensor (14) exclusively in cones. All procedures were previously published (15). In brief, dark-adapted (≥2 h) mice were anesthetized and killed by decapitation (until P10) or cervical dislocation. Eyes were enucleated and dissected in artificial cerebrospinal fluid (ACSF) solution containing (in millimolar) 125 NaCl, 2.5 KCl, 2 $CaCl_2$, 1 $MgCl_2$, 1.25 NaH_2PO_4, 26 $NaHCO_3$, 0.5 L-glutamine, and 20 mM glucose (pH 7.4), bubbled with carboxygen (95% O_2, 5% CO_2). Acute, 200-μm-thick vertical slices were cut and moved to the recording chamber of a two-photon microscope, where they were constantly perfused with carboxygenated ACSF at 37 °C. All CN compounds were freshly dissolved in water and bath-applied with a final compound concentration of ∼50 μM for at least 10 min, at a perfusion rate of ∼2 mL/min.

Ca^{2+} imaging was performed on a MOM-type two-photon microscope [designed by W. Denk, MPI Neurobiology, Martinsried (16) and purchased by Sutter Instruments]. The system consisted of a mode-locked Ti:sapphire laser (MaiTai-HP DeepSee; Newport Spectra-Physics GmbH) tuned to 860 nm, using two channels for the detection of enhanced cyan fluorescent protein (483 BP 32; AHF) and citrine (535 BP 50) fluorescence, and a 20× water immersion objective (XLUMPlanFL, 0.95 N.A.; Olympus). Images were acquired with custom-made software (ScanM by M. Müller, MPI Neurobiology, Martinsried and T. Euler, CIN), as 128- × 16-pixel image sequences at 31.25 frames per s. The custom-built light stimulator (17) consisted of two band-pass-filtered (blue: 360 BP 12, green: 578 BP 10; AHF) LEDs driven by an Arduino board (arduino.cc). Slices were adapted to a constant background illumination of 10^4 $P{\cdot}s^{-1}$ (photoisomerization rate) for 15–20 s, before light stimulation. During light stimulation, bright "mouse-white" 1-s flashes with 4-s intervals were projected on the slices for ≥12 trials (for details see ref. 18).

Ca^{2+} data were processed and analyzed in IGOR Pro-6.3 (Wavemetrics). Regions of interest (ROIs) were drawn around the cone axon terminals and pixels were averaged from each frame of selected ROIs. A ROI drawn outside the OPL was used for background subtraction, then relative Ca^{2+} levels were calculated as the ratio (R) between acceptor and donor fluorescence (F_A/F_D) signals. Stimulus trials were averaged and relative resting Ca^{2+} level (R_{base}) was determined by calculating the mean of a 0.5-s trace before stimulus onset. Only cones showing light evoked activity under control condition (ACSF) were used for statistical analysis.

PK Studies in Rats. A PK study was performed at WIL Research using a single 20 mg/kg dose of either CN03 or LP-CN03 administered i.v. into the tail vein of male Wistar rats (n = 6 per group, 8–10 wk old) at a rate of 1 mL/min. Approximately 0.3-mL blood samples were taken from the jugular vein and collected into tubes containing Li-heparin (Greiner Bio-One GmbH) as anticoagulant. Blood samples were taken from three animals per group at 5 min, 30 min, 2 h, and 8 h after injection. In the other three animals per group blood samples were taken at 15 min, 1 h, 4 h, and 24 h after injection. Blood samples were stored on ice until centrifugation within a maximum of 2 h after sampling, after which plasma was stored in labeled polypropylene tubes (Greiner Bio-One GmbH) at approximately ≤−75 °C until further analysis.

A standard for CN03 was generated by spiking 0.78–200 μg/mL CN03 in heparinized plasma from untreated rats. All plasma samples were thawed and subsequently precipitated with 100% methanol 1:2 (vol/vol), vortexed, and pelleted for 10 min at 5,000 × g. CN03 recovery from plasma was assessed by spiking 0.78–200 μg/mL CN03 in methanol-extracted plasma from untreated rats. Supernatants were subjected to CN03 analysis using HPLC. LP-CN03 samples were diluted in 25% acetonitrile/75% MilliQ (vol/vol) for CN03 analysis or in 100% methanol for lipid and cholesterol analysis. A standard curve comprising 100–0.78 μg/mL CN03 was made in 25% ACN/75% MilliQ (vol/vol). Ten microliters was injected on a Kinetix 2.6 μm, XB-C18, 100 Å, 150- × 4.6-mm column (Phenomenex) for separation. The mobile phase consisted of buffer A (50 mM NaH_2PO_4) and buffer B (100% acetonitrile). CN03 was eluted in an isocratic manner with 76% buffer A and 24% buffer B at a flow rate of 1 mL/min. CN03 was detected at a wavelength of 256 nm. Data were processed using TotalChrom navigator v 6.3.2 (PerkinElmer).

Drug Testing in RD Models in Vivo. Before treatment with drug or drug/drug delivery system combinations the animals were briefly anesthetized with diethyl ether (Merck KGaA). For treatment 0.9% NaCl solution containing CN03/LP-CN03 was injected into the peritoneum i.p. (200 μL).

The in vivo CN03/LP-CN03 treatment was performed initially on *rd1* animals but later extended to other animal models (*rd2* and *rd10*). To determine the minimal number of animals required to allow for successful in vivo testing, a biometric expertise was obtained from the Tübingen University Institute for Clinical Epidemiology and Applied Biometry. Here, the key criterion for determining appropriate sample sizes was the SD on ERG recordings. For each experiment two litters with four animals each were used; the allocation of animals to experimental groups was not randomized. Because of the different onset and progression of RD in the different RD models the treatment paradigms had to be adapted to each model. For details on these treatment paradigms see Table S2.

For noninvasive in vivo testing the animals were anesthetized using i.p. injection of 100 mg/kg body weight ketamine (Bela-Pharm) and 5 mg/kg xylazine (Bayer Vital); 0.5% oxybuprocaine solution (Omnivision) was used for local anesthesia of the eye and 0.5% tropicamide (Pharma Stulln GmbH) for pupillary dilation. At various posttreatment time points (Table 2) in vivo retinal function was assessed after 12-h dark adaptation using ERG recordings with cotton wick electrodes (19) and an Espion e^2 system with a Ganzfeld stimulator (Diagnosys UK Ltd) using an extended International Society for Clinical Electrophysiology of Vision (ISCEV) protocol (20, 21). For details on the ERG protocol see Table S3. The a-wave (i.e., the primary photoreceptor response) and the b-wave (i.e., the response of second order neurons in the inner retina) were processed and exported using custom-developed software (22) for subsequent statistical analysis (discussed below). ERG recording was followed by in vivo optic coherence tomography (OCT) and SLO analysis for direct, noninvasive imaging of retinal morphology, using a Spectralis HRA + OCT (Heidelberg Engineering GmbH).

After the last in vivo examination, experimental animals were killed by carbon dioxide asphyxiation. The eyes were immediately enucleated, fixated for 2 h in 4% PFA, and prepared for cryosectioning. Using a Zeiss Axioskop microscope equipped with a Zeiss Axiocam TRm digital camera, images of DAPI-stained sagittal retinal sections were captured for each experimental animal and used to count the number of surviving photoreceptor rows. The photoreceptor row count was assessed along the dorsoventral axis at 12 different positions, at plus and minus 5, 10, 20, 40, 60, and 80°, as seen from the optic nerve (0°). For each

position, six vertical lines were drawn across the ONL and the number of ONL nuclei touching the line was counted. These six individual counts were averaged to give the photoreceptor row count for the corresponding position and animal.

Statistics.

Photoreceptor-like cell cultures. For statistical analysis Prism 7.04 software (GraphPad Software) was employed. To test for the effects of the various cGMP analogs on photoreceptor-like cells, a one-way ANOVA followed by Holm–Šidak's multiple-comparisons test was performed. The effects of liposome (LP) vs. free CN03 vs. LP-CN03 were tested using a one-way ANOVA and Newman–Keuls multiple comparison, for one-to-one comparisons (untreated vs. treated) Student's *t* test was used. Levels of significance were $^{*}P < 0.05$, $^{**}P < 0.01$, and $^{***}P < 0.001$.

TUNEL counts in retinal explant cultures. Evaluation covering all tested analogs was performed using Prism 7.04 software (GraphPad Software) and ANOVA testing, followed by Holm–Sidak's multiple-comparisons test. For one-to-one comparisons (untreated vs. treated) Student's *t* test as implemented in Prism 7.03 was used.

Ca^{2+} imaging data. Comparison of WT NT and compound treated effects was analyzed using Prism 7.04 software (GraphPad software) and Wilcoxon matched-pairs signed rank test.

ERG data analysis. A one-way between-treatments ANOVA (untreated, LP-CN03, and empty liposome) was conducted for a- and b-wave ERG amplitudes for all stimulus intensities as well as for the Fourier-transformed flicker magnitudes, to compare the effect of LP-CN03 on retinal function. Results of the single ANOVAs are listed in Table 2. For statistically significant effects, post hoc comparison was performed using Tukey's honestly significant difference test (Table 3). ERG analyses were conducted using JMP software (version 12.2.0; SAS Institute Inc.).

Ex vivo photoreceptor row counts. For statistical comparisons the unpaired, two-tailed Student's *t* test as implemented in Prism 7.04 (GraphPad Software) was employed.

1. Genieser HG, Walter U, Butt E (1997) Derivatives of cyclic guanosine-3′,5′-monophosphorothioate. US Patent 5,625,056.
2. Butt E, Pöhler D, Genieser HG, Huggins JP, Bucher B (1995) Inhibition of cyclic GMP-dependent protein kinase-mediated effects by (Rp)-8-bromo-PET-cyclic GMPS. *Br J Pharmacol* 116:3110–3116.
3. Krass JD, Jastorff B, Genieser HG (1997) Determination of lipophilicity by gradient elution high-performance liquid chromatography. *Anal Chem* 69:2575–2581.
4. Werner K, Schwede F, Genieser HG, Geiger J, Butt E (2011) Quantification of cAMP and cGMP analogs in intact cells: Pitfalls in enzyme immunoassays for cyclic nucleotides. *Naunyn Schmiedebergs Arch Pharmacol* 384:169–176.
5. Giordano F, De Marzo A, Vetrini F, Marigo V (2007) Fibroblast growth factor and epidermal growth factor differently affect differentiation of murine retinal stem cells in vitro. *Mol Vis* 13:1842–1850.
6. Sanges D, Comitato A, Tammaro R, Marigo V (2006) Apoptosis in retinal degeneration involves cross-talk between apoptosis-inducing factor (AIF) and caspase-12 and is blocked by calpain inhibitors. *Proc Natl Acad Sci USA* 103: 17366–17371.
7. Demontis GC, Aruta C, Comitato A, De Marzo A, Marigo V (2012) Functional and molecular characterization of rod-like cells from retinal stem cells derived from the adult ciliary epithelium. *PLoS One* 7:e33338.
8. Caffé AR, et al. (2001) Mouse retina explants after long-term culture in serum free medium. *J Chem Neuroanat* 22:263–273.
9. Romijn HJ (1988) Development and advantages of serum-free, chemically defined nutrient media for culturing of nerve tissue. *Biol Cell* 63:263–268.
10. Sahaboglu A, et al. (2016) Olaparib significantly delays photoreceptor loss in a model for hereditary retinal degeneration. *Sci Rep* 6:39537.
11. Hauck SM, et al. (2006) Differential modification of phosducin protein in degenerating rd1 retina is associated with constitutively active Ca2+/calmodulin kinase II in rod outer segments. *Mol Cell Proteomics* 5:324–336.
12. Schindelin J, et al. (2012) Fiji: An open-source platform for biological-image analysis. *Nat Methods* 9:676–682.
13. Wei T, et al. (2012) Light-driven calcium signals in mouse cone photoreceptors. *J Neurosci* 32:6981–6994.
14. Mank M, et al. (2006) A FRET-based calcium biosensor with fast signal kinetics and high fluorescence change. *Biophys J* 90:1790–1796.
15. Kulkarni M, et al. (2015) Imaging Ca2+ dynamics in cone photoreceptor axon terminals of the mouse retina. *J Vis Exp* e52588.
16. Euler T, et al. (2009) Eyecup scope—Optical recordings of light stimulus-evoked fluorescence signals in the retina. *Pflugers Arch* 457:1393–1414.
17. Breuninger T, Puller C, Haverkamp S, Euler T (2011) Chromatic bipolar cell pathways in the mouse retina. *J Neurosci* 31:6504–6517.
18. Kulkarni M, Trifunović D, Schubert T, Euler T, Paquet-Durand F (2016) Calcium dynamics change in degenerating cone photoreceptors. *Hum Mol Genet* 25:3729–3740.
19. Chekroud K, et al. (2011) Simple and efficient: Validation of a cotton wick electrode for animal electroretinography. *Ophthalmic Res* 45:174–179.
20. McCulloch DL, et al. (2015) ISCEV Standard for full-field clinical electroretinography (2015 update). *Doc Ophthalmol* 130:1–12.
21. Tanimoto N, et al. (2015) Electroretinographic assessment of rod- and cone-mediated bipolar cell pathways using flicker stimuli in mice. *Sci Rep* 5:10731.
22. Strasser T, Peters T, Jagle H, Zrenner E, Wilke R (2010) An integrated domain specific language for post-processing and visualizing electrophysiological signals in Java. *Conf Proc IEEE Eng Med Biol Soc* 2010:4687–4690.

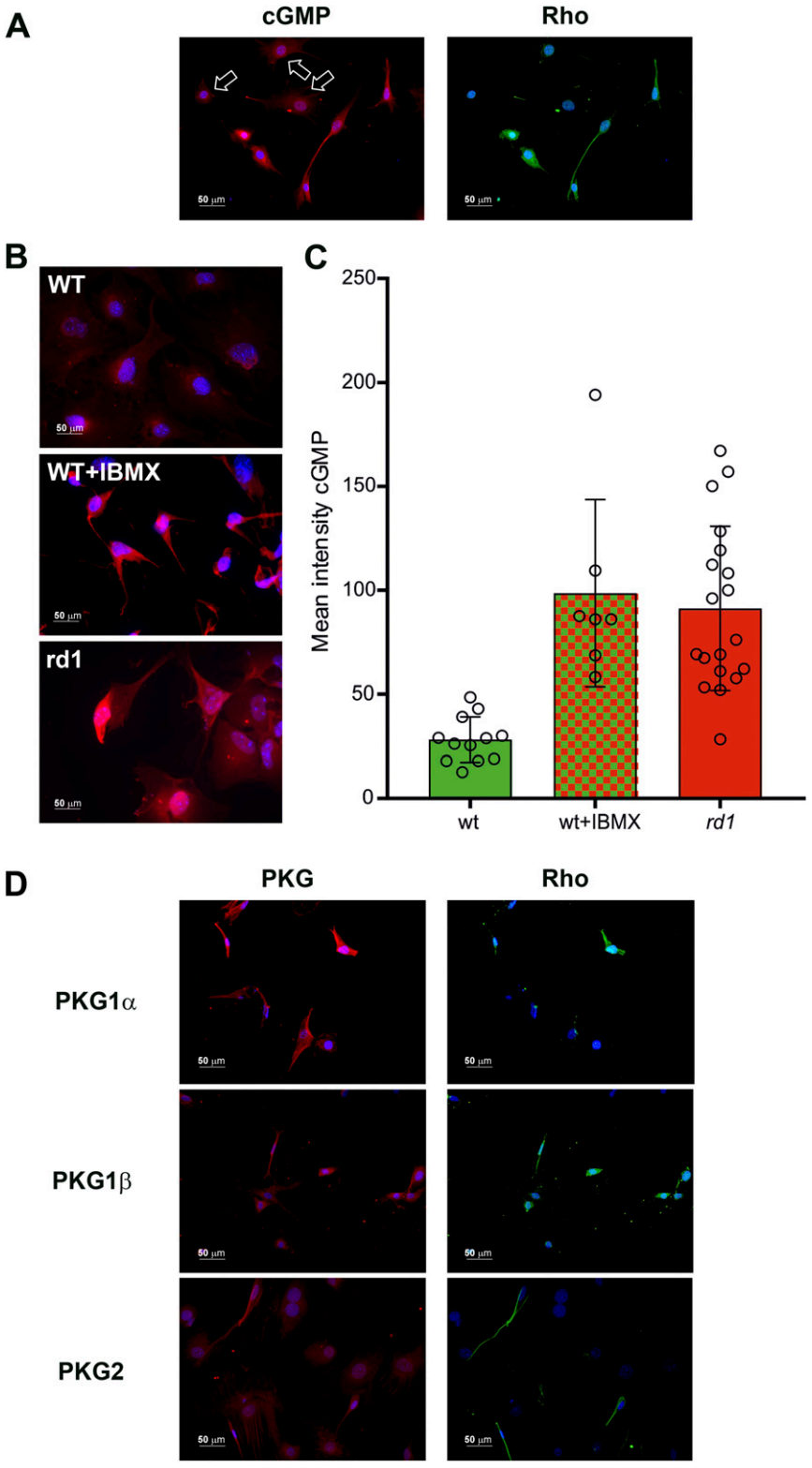

Fig. S1. cGMP accumulation and PKG expression in photoreceptor-like cells. Photoreceptor-like cells were differentiated from retinal neurospheres derived from either WT or *rd1* mutant eyes. *rd1* mutant photoreceptors undergo spontaneous cell death with a peak at the 11th day (DIV11) of differentiation (1). (*A*) *rd1* mutant cells were coimmunostained for cGMP (red) and rhodopsin (green) at DIV11. The red and green channels are shown in two separate panels and DAPI (blue) was used as a nuclear counterstain. High cGMP staining was observed only in cells expressing rhodopsin and not in other cells (open arrows). (*B*) *rd1*- and WT-derived cells were immunostained at DIV11 for cGMP (red) and DAPI (blue) was used as a nuclear counterstain. WT cell cultures treated for 1 h with the PDE inhibitor IBMX (2 mM) showed a strong intracellular accumulation of cGMP, similar to what was observed in *rd1*-derived cell cultures in the absence of IBMX. (*C*) cGMP accumulation was assessed by analyzing fluorescence intensity in the red channel with ImageJ software. Error bars: SEM, $n = 7$–19 cells obtained from three independent primary cell preparations. (*D*) *rd1* mutant cells were immunostained for the three PKG isoforms (PKG1α, PKG1β, and

Legend continued on following page

PKG2) in red and for rhodopsin in green. DAPI (blue) was used as a nuclear counterstain. Rhodopsin-positive cells, as well as other retinal cells, expressed all of the three PKG isoforms.

1. Sanges D, Comitato A, Tammaro R, Marigo V (2006) Apoptosis in retinal degeneration involves cross-talk between apoptosis-inducing factor (AIF) and caspase-12 and is blocked by calpain inhibitors. *Proc Natl Acad Sci USA* 103:17366–17371.

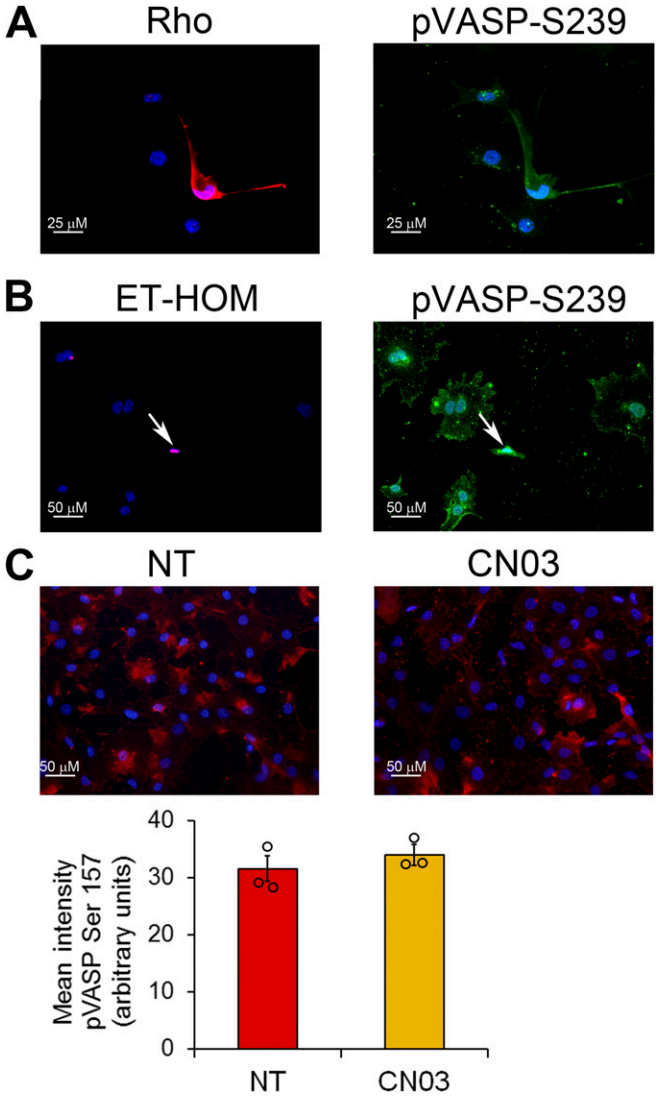

Fig. S2. VASP phosphorylation analysis. Photoreceptor-like cells were differentiated from retinal neurospheres derived from *rd1* mutant eyes. *rd1* mutant photoreceptors undergo spontaneous cell death with a peak at the 11th day (DIV11) of differentiation (1). (*A*) *rd1* mutant cells were immunostained at DIV11 for rhodopsin (red) and pVASP at Ser239 (green). Nuclei were counterstained in blue with DAPI. The rhodopsin-positive cells showed high VASP phosphorylation at Ser239. (*B*) Cells undergoing cell death were stained with ethidium homodimer (red) and for phosphorylated VASP at Ser239 (green) at DIV11. Nuclei were counterstained with DAPI (blue). High phosphorylated VASP at Ser239 was observed in ethidium-positive cells (arrow). (*C*) To confirm that CN03 targets PKG and not PKA we analyzed VASP phosphorylation at Ser157 in *rd1* mutant cells treated or not treated (NT) at DIV10 with 50 μM CN03. At DIV11, cells were immunostained for phosphorylated VASP at Ser157 (red) and counterstained with DAPI (blue). No changes in VASP phosphorylation at Ser157 were observed after CN03 treatment as assessed by analyzing fluorescence intensity in the red channel with ImageJ software, indicating that CN03 specifically targets PKG. Error bars: SEM, $n = 3$ measurements from three independent primary cell preparations.

1. Sanges D, Comitato A, Tammaro R, Marigo V (2006) Apoptosis in retinal degeneration involves cross-talk between apoptosis-inducing factor (AIF) and caspase-12 and is blocked by calpain inhibitors. *Proc Natl Acad Sci USA* 103:17366–17371.

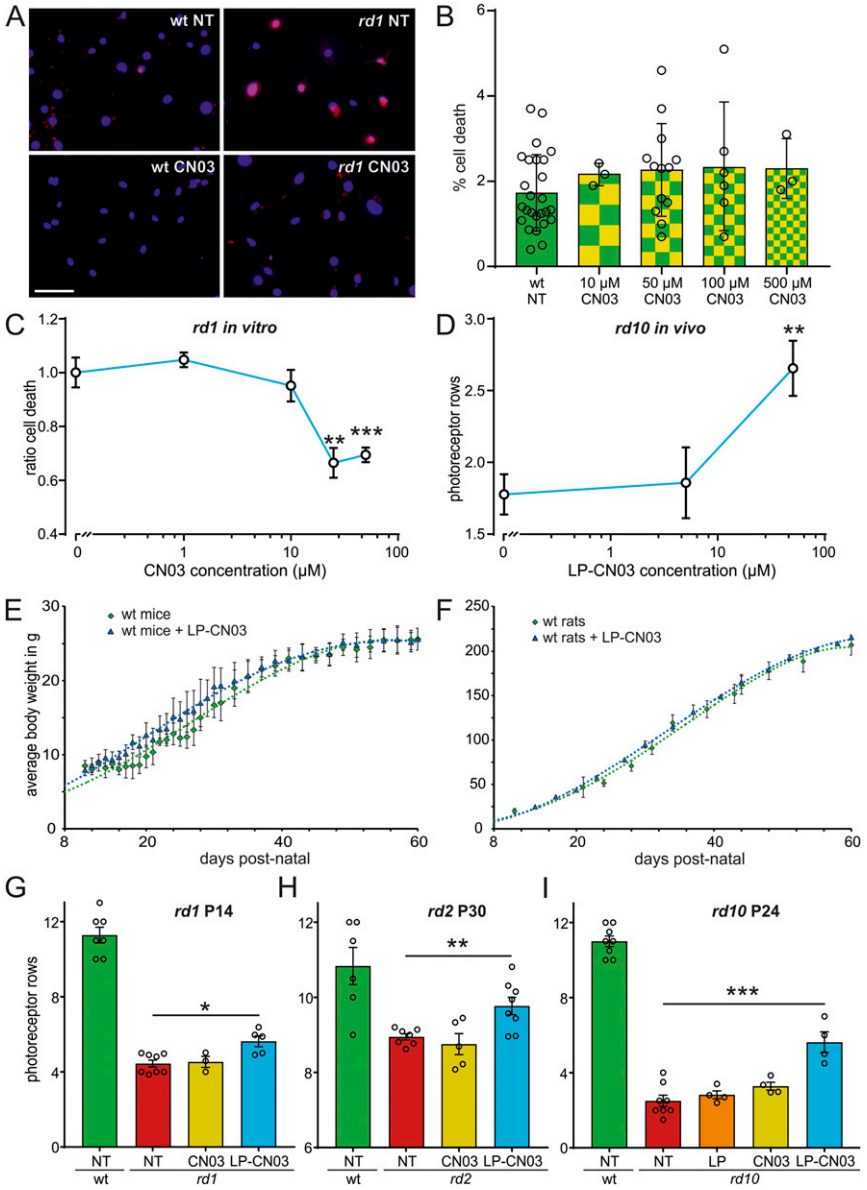

Fig. S3. Evaluation of CN03 safety and efficacy. (*A*) Micrographs of photoreceptor-like cells derived from WT and *rd1* neurospheres, CN03-treated or not treated (NT). Cell nuclei were stained with DAPI (blue) and dying cells with ethidium homodimer (red). (*B*) WT cell cultures exposed to CN03 at concentrations of up to 500 µM did not show any significant changes in cell death compared with NT. (*C*) In *rd1* in vitro retinal explant cultures decreased cell death was observed at CN03 concentrations from 25 to 50 µM. $n = 12$ separate *rd1* explant cultures for NT (0 µM), 4 for 1 µM, 4 for 10 µM, 6 for 25 µM, and 8 for 50 µM. (*D*) After in vivo LP-CN03 treatment P30 *rd10* animals showed a concentration-dependent increase in surviving photoreceptor rows. $n = 8$ animals for NT, 4 for 5 µM, and 8 for 50 µM. (*E*) Untreated WT mice (green diamonds, four males, four females) increased their body weights from 8 g to about 25 g during the first two postnatal months. Treatment with LP-CN03 (i.p. injections every second day, 200 µL from day 11–29 and 300 µL from day 31–59; blue triangles) did not affect these weight gains ($n = 7$–8 mice per time point). (*F*) Untreated WT rats (females only; green diamonds) gained from 20 g to about 215 g in 2 mo. Rats that had received LP-CN03 every fourth day (400 µL from day 14–18,; 800 µL from day 22–28, and 1.2 mL from day 32–58; blue triangles) showed no alterations in weight gains compared with control ($n = 4$–6 rats per time point). (*G–I*) *rd1*, *rd2*, and *rd10* animals treated with CN03, LP only, or LP-CN03. Photoreceptor survival analyzed as in *D*. WT (green) shown for comparison. $n = 3$–8 animals (one eye per animal) per time point and genotype. Data are shown for time points when the largest treatment effect was observed (cf. Fig. 5). (*G*) P14 photoreceptor row counts in *rd1* animals (red) compared with *rd1* animals treated with free CN03 (yellow) and LP-CN03 (blue). (*H* and *I*) Same analysis as in *G* but for P30 *rd2* retina and P24 *rd10* retina, respectively. For *rd10* with additional comparison with empty liposome (LP, orange). Note different *y*-axis scales in *G–I* to account for different degeneration kinetics. Error bars: SEM; dotted lines in *E* and *F* represent polynomial regression fits; statistical comparisons: *C* and *D*, NT-*rd1*/*rd10* vs. treated, using one-way ANOVA with Holm–Šidak's multiple-comparisons test. *G–I*, Student's *t* test (unpaired, two-tailed). Note that the 50 µM values (*C* and *D*) and some (*C*) or all (*D*) NT values were used in Figs. 2*G* and 5*I*, respectively. $*P \leq 0.05$, $**P \leq 0.01$, $***P \leq 0.001$.

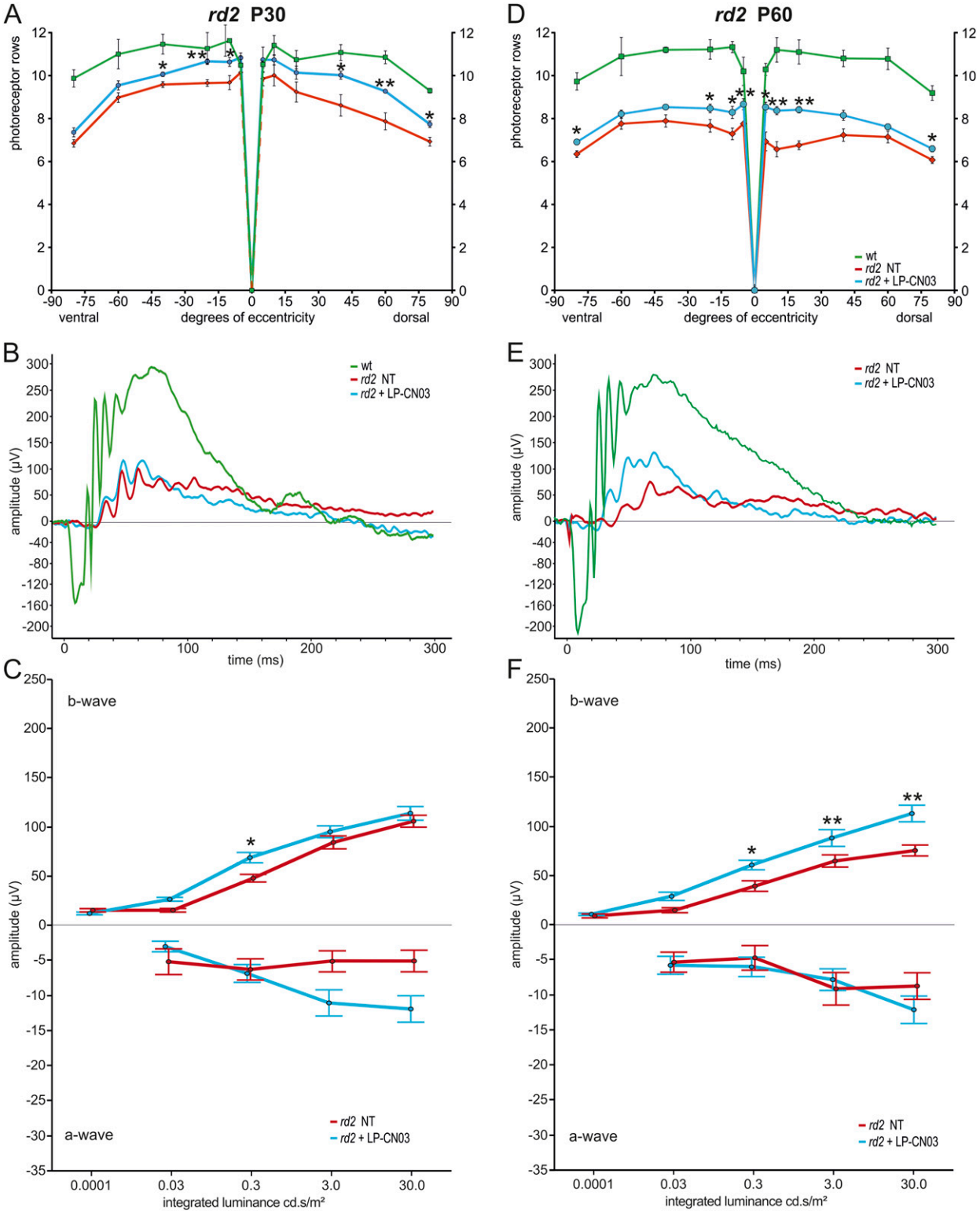

Fig. S4. LP-CN03 treatment delays *rd2* photoreceptor loss and preserves retinal function. (*A*) At P30 a photoreceptor row count across the entire dorsoventral axis shows that not treated (NT) *rd2* retina (red) had lost between 10–20% of its photoreceptors. In contrast, in LP-CN03 treated retina (blue) photoreceptor loss was significantly reduced. WT photoreceptor row counts shown for comparison (green). (*B*) Representative ERG traces obtained from WT, NT, and LP-CN03–treated *rd2* animals. (*C*) Average ERG b-wave (positive deflection, *Top*) and a-wave amplitudes (negative deflection, *Bottom*). LP-CN03 treatment resulted in increased b-wave responses; this effect was significant at a light level of 0.3 cd·s/m^2. a-wave responses in *rd2* animals were always very small, close to the noise level, likely due to the *Prph2* mutation and the resultant absence of rod and cone outer segments. (*D*–*F*) Analysis as in *A*–*C* but for P60 *rd2* retina. (*D*) *rd2* photoreceptor numbers decreased, compared with P30. Photoreceptor loss was significantly reduced in LP-CN03–treated animals. (*E*) Representative ERG traces showing that b-wave responses in treated *rd2* animals were essentially preserved at the P30 level (cf. *B*), while strongly deteriorating in NT. (*F*) P60 statistical analysis confirmed a preservation of b-wave responses after LP-CN03 treatment, while NT animals performed significantly worse than at P30

Legend continued on following page

(cf. *C*). P30, P60: $n = 3$ for WT, $n = 8$ for NT *rd2* and *rd2* + LP-CN03. Error bars in *A*–*F*: SEM; Student's *t*-test (unpaired, two-tailed) used for analysis in *A* and *D*; one-way ANOVA with Tukey's honestly significant difference post hoc test used in *C* and *F*; significance levels: $^{*}P < 0.05$, $^{**}P < 0.01$, $^{***}P < 0.001$.

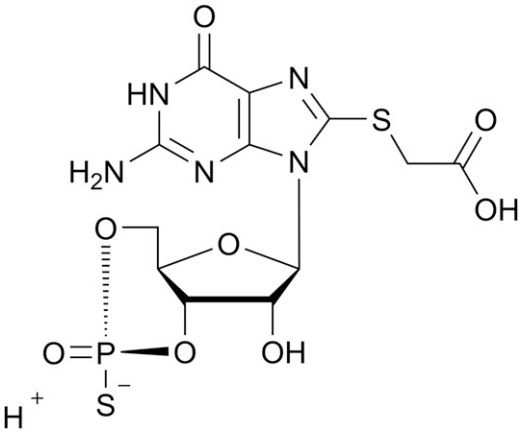

Fig. S5. Precursor for synthesis of CN09: 8-carboxymethylthioguanosine-3′,5′-cyclic monophosphorothioate, R_P-isomer (R_P-8-CMT-cGMPS).

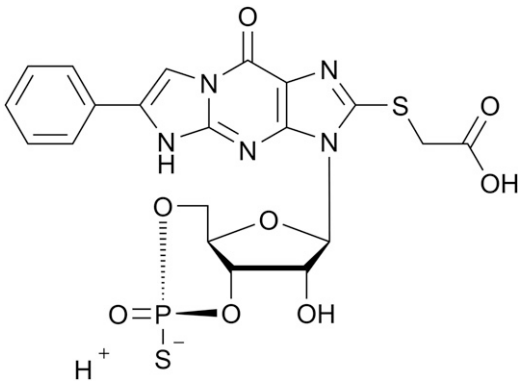

Fig. S6. Precursor for synthesis of CN10: 8-carboxymethylthio-β-phenyl-1,N^2-ethenoguanosine- 3′,5′-cyclic monophosphorothioate, R_P-isomer (R_P-8-CMT-PET-cGMPS).

Table S1. Compound codes, acronyms, and nomenclature names

Code	Acronym	Compound name
A	cGMP	Guanosine-3′,5′-cyclic monophosphate
B	R_P-cGMPS	Guanosine-3′,5′-cyclic monophosphorothioate, R_P-isomer
C	R_P-8-Br-cGMPS	8-bromoguanosine-3′,5′-cyclic monophosphorothioate, R_P-isomer
CN01	8-pCPT-cGMP	8-(4-chlorophenylthio)guanosine-3′,5′-cyclic monophosphate
CN02	R_P-8-pCPT-cGMPS	8-(4-chlorophenylthio)guanosine-3′,5′-cyclic monophosphorothioate, R_P-isomer
CN03	R_P-8-Br-PET-cGMPS	8-bromo-β-phenyl-1,N^2-ethenoguanosine-3′,5′-cyclic monophosphorothioate, R_P-isomer
CN04	R_P-8-pCPT-PET-cGMPS	8-(4-chlorophenylthio)-β-phenyl-1,N^2-ethenoguanosine-3′,5′-cyclic monophosphorothioate, R_P-isomer
CN05	R_P-8-pHPT-PET-cGMPS	8-(4- hydroxyphenylthio)-β-phenyl-1,N^2-ethenoguanosine-3′,5′-cyclic monophosphorothioate, R_P-isomer
CN06	R_P-8-pIPrPT-PET-cGMPS	8-(4-isopropylphenylthio)-β-phenyl-1,N^2-ethenoguanosine-3′,5′-cyclic monophosphorothioate, R_P - isomer
CN07	R_P-8-Br-(3-Tp)ET-cGMPS	8-bromo-(3-thiophen-yl-1,N^2-etheno)guanosine-3′,5′-cyclic monophosphorothioate, R_P-isomer
CN08	R_P-8-oAPT-cGMPS	8-(2-aminophenylthio)guanosine-3′,5′-cyclic monophosphorothioate, R_P-isomer
Precursor for synthesis of CN09	R_P-8-CMT-cGMPS	8-carboxymethylthioguanosine-3′,5′-cyclic monophosphorothioate, R_P-isomer
CN09	R_P-cGMPS-8-TMAmd-$(EO)_8$-EAmdMT-8- R_P-cGMPS	Guanosine-3′,5′-cyclic monophosphorothioate[R_P]-[8-thiomethylamido-(octaethoxy)-ethylamidomethylthio-8]-guanosine-3′,5′-cyclic monophosphorothioate[R_P]
Precursor for synthesis of CN10	R_P-8-CMT-PET-cGMPS	8-carboxymethylthio-β-phenyl-1,N^2-ethenoguanosine-3′,5′-cyclic monophosphorothioate, R_P-isomer
CN10	PET- R_P-cGMPS-8-TMAmd-$(EO)_8$-EAmdMT-8- R_P-cGMPS-PET	β-Phenyl-1,N^2-ethenoguanosine-3′,5′-cyclic monophosphorothioate[R_P]-[8-thiomethylamido-(octaethoxy)-ethylamidomethylthio-8]-β-phenyl-1,N^2-ethenoguanosine-3′,5′-cyclic monophosphorothioate[R_P]

Table S2. RD models used and in vivo treatment paradigms

Animal model: gene and ref.	Treatment start	Treatment interval/dose	Treatment end	In vivo analysis
rd1 mouse: *Pde6b* (1)	P10	Once per day/200 μL (~50 mg/kg)	PN13	P14
rd2 mouse: *Prph2* (2)	P14	Every second day/200–300 μL (~25 mg/kg)	PN59	P30, 60
rd10 mouse: *Pde6b* (3)	P14	Once per day/200 μL (~25 mg/kg)	PN29	P30

1. Sanyal S, Bal AK (1973) Comparative light and electron microscopic study of retinal histogenesis in normal and rd mutant mice. *Z Anat Entwicklungsgesch* 142:219–238.
2. Sanyal S, Hawkins RK (1981) Genetic interaction in the retinal degeneration of mice. *Exp Eye Res* 33:213–222.
3. Chang B, et al. (2002) Retinal degeneration mutants in the mouse. *Vision Res* 42:517–525.

Table S3. Modified ISCEV ERG protocol, extended with a flicker series

Step	Stimulus	Flicker frequency, Hz	Stimulus intensity, cd·s/m^2	Background luminance, cd/m^2	Sampling frequency, kHz	Recording time, ms	Sweeps	Intersweep delay, s	Adaptation time, s
12-h dark adaptation									
1	Flash		0.0001*	Off	1	300	8	10	
2	Flash		0.003*	Off	1	300	8	10	
3	Flicker	5.0	0.003*	Off	2	2,000	16	10	30
4	Flash		0.3*	Off	1	300	4	20	
5	Flash		3.0*	Off	1	300	4	20	
6	Flash		30.0*	Off	1	300	4	20	
5-min light adaptation (30.0† cd/m^2, 6,500 K)									
7	Flash		3.0†	30.0	1	200	10	1	
8	Flicker	5.0	30.0†	30.0	2	1,000	16		40
9	Flicker	10.0	30.0†	30.0	2	500	16		40
10	Flicker	15.0	30.0†	30.0	2	700	16		40
11	Flicker	20.0	30.0†	30.0	2	500	16		40
12	Flicker	31.25	30.0†	30.0	2	320	16		40

Single flash duration ≤4 ms; recordings filtered using a band-pass filter (0.321–300 Hz); flicker ERG: linear drift removal; single flash ERG: baseline removal using a 20-ms pretrigger time.
*Scotopic candela.
†Photopic candela.